Photophysiological variability and its influence on primary production in the NW Africa-Canary Islands coastal transition zone

F.G. Figueiras [a, *], B. Arbones [a], M.F. Montero [b], E. D. Barton [a], J. Arístegui [b]

[a] Instituto de Investigacións Mariñas, CSIC, Eduardo Cabello 6, 36208 Vigo, Spain

[b] Instituto de Oceanografía y Cambio Global (IOCAG), Universidad de Las Palmas de Gran Canaria, 35017 Las Palmas de Gran Canaria, Spain.

[*]Corresponding author

E-mail: paco@iim.csic.es

Tel: +34 986 231 930

Fax: + 34 986 292 762

ABSTRACT

Photophysiological variability and its influence on primary production were studied in the NW Africa-Canary Islands coastal transition zone. The region showed strong mesoscale activity, in which upwelling filaments and island eddies interacted to cause significant vertical displacements of the deep chlorophyll maximum (DCM). Oligotrophic stations both in the open ocean and within anticyclonic eddies were characterized by low values of integrated chlorophyll (33 ± 4 mg chl *a* m^{-2}) and dominance of pico- and nanophytoplankton, while stations associated with filaments and cyclonic eddies showed moderate chl *a* values (50 ± 17 mg m^{-2}). Shelf stations affected by upwelling exhibited the highest chl *a* (112 ± 36 mg m^{-2}) with microphytoplankton dominance. Photosynthetic variables in the three groups of stations showed similar depth gradients, with maximum photosynthetic rates (P_m^B) decreasing with depth and maximum quantum yields (ϕ_m) increasing with depth. However, the increase with depth of ϕ_m was not so evident in shelf waters where nutrients were not depleted at surface. Primary production (PP) displayed a coast-ocean gradient similar to that of chl *a*, with highest values (2.5 ± 1.2 g C m^{-2} d^{-1}) at the eutrophic shelf stations and lowest (0.36 ± 0.11 g C m^{-2} d^{-1}) at the oligotrophic stations. Nevertheless, integrated PP at the oligotrophic stations was not related to integrated chl *a* concentration but was positively (r = 0.95) correlated to carbon fixation at the DCM and negatively (r = -0.85) correlated to the depth of the DCM, suggesting that light, and not phytoplankton biomass, was the main factor controlling PP in oligotrophic environments. It is concluded that downward displacements of the DCM, either by convergence fronts or downwelling at the core of anticyclones can significantly reduce PP in the oligotrophic ocean.

Keywords: Phytoplankton; photosynthetic response; light limitation; anticyclonic eddies; Canary Islands; NW Africa upwelling.

1. Introduction

Mesoscale structures such as fronts, filaments and eddies in the surface layer of the ocean affect phytoplankton distribution and, consequently, influence carbon fixation and the fate of the organic material produced. Thus, dispersion is largely reduced in fronts, where cells accumulate and the phytoplankton community is restructured splitting populations in space (Pingree et al., 1975). Filaments also reorganize the spatial distributions in coastal upwelling systems while transporting plankton populations from the shelf to the nearby oligotrophic ocean (Joint et al., 2001; Arístegui et al., 2004). Large vertical displacements are among the most obvious effects imposed by eddies on phytoplankton in the stratified oligotrophic ocean (Basterretxea et al., 2002; Brown et al., 2008). Cyclonic eddies can uplift the thermocline and the associated deep chlorophyll maximum (DCM) to a light level where photosynthesis is neither light nor nutrient limited and phytoplankton growth is stimulated (Falkowski et al., 1991; Arístegui et al., 1997; McGillicuddy et al., 1998), whereas the DCM can be moved below the photic layer in anticyclonic eddies (McGillicuddy et al., 1998; Basterretxea et al., 2002). While the influence of cyclonic eddies on phytoplankton (Arístegui et al., 1997; Vaillancourt et al., 2003; Brown et al., 2008) and primary production (Falkowski et al., 1991; McGillicuddy et al., 1998; McAndrew et al., 2008) has been widely documented; the effect of anticyclonic eddies on phytoplankton photosynthesis still needs to be typified. Therefore, it is important to know the photophysiological response of phytoplankton in these mesoscale structures for improving estimates of primary production and better characterise carbon fluxes in oceanic regions with strong eddy influence.

The NW Africa-Canary Islands coastal transition zone is a region with intense mesoscale activity where eddies are ubiquitous (Barton et al., 1998; 2004). In addition to the variability imposed by upwelling on the African shelf from where filaments develop and progress (Barton et al., 2004), the Canary Islands generate another type of variability. The archipelago perturbs the flow of both the Canary Current and the Trade winds (Arístegui et al. 1994; Barton et al., 1998; Sangrà et al., 2009), leading to the formation of eddies that are shed downstream from the islands. The perturbation of the Canary Current seems to be the main source for eddy generation, since eddies have been observed in the region even in winter, when wind intensity is very low (Arístegui et al., 1994; Rodríguez et al. 1999; Piedeleu et al., 2009). Consequently, the region represents a continuous source of eddies that can remain as coherent structures for several months (Sangrà et al., 2005, 2007) while they are propagated westward (Sangrà et al., 2009). Although cyclones and anticyclones are detached from all islands, anticyclones shed from Gran Canaria and Tenerife persists longer, probably due to higher initial intensity and later interaction with other eddies (Sangrà et al., 2009).

The goal of this study was to look at the effects that convergent and divergent processes associated with eddies and filaments have on photophysiological activity of phytoplankton and in turn on primary production. Particularly, we aimed at understanding the effect that light has on the photosynthetic efficiency of phytoplankton forming deep chlorophyll maxima in oligotrophic environments, across the NW Africa-Canary Islands coastal transition zone. Carbon fixation in these chlorophyll maxima accounts for an important fraction of the total water column integrated primary production (e.g. Lorenzo et al. 2004), but these maxima are usually found at the bottom of the euphotic zone coinciding with the nutricline (Cullen, 2015). Therefore, it is

hypothesised that light is the main environmental factor regulating carbon fixation in these environments.

2. Materials and methods

2.1. Sampling

The NW Africa-Canary Islands costal transition zone was visited from 5 to 27 August 1999 on board the R/V *Hesperides* (Fig. 1). Sampling began at the station located northwest of the island of La Palma and continued along the long line that ended in front of Cape Juby on the African coast. Then, several sections crossing the filaments and eddies present in the transition zone were sampled. Note that structures seen in the image of Fig. 1 do not necessarily coincide in position with those sampled at the stations because the eddy field evolved significantly during the 3-week cruise.

Vertical profiles of temperature, salinity and fluorescence were recorded with a Neil Brown Mk III conductivity-temperature-depth (CTD) probe and a Sea-Tech fluorometer mounted on a General Oceanics rosette equipped with twenty four 12 L PVC Niskin bottles. Biological and bio-optical variables were determined at 31 stations throughout the sampling area (Fig. 1). At these stations, samples were taken from the CTD upcasts to determine nitrate and chlorophyll *a* (chl *a*) concentrations and characterise the photophysiological performance of phytoplankton community. Phytoplankton biomass was determined at several of these stations. Sampling depths were selected after inspecting the downward profiles of fluorescence. Nitrate and chl *a* concentrations were determined at 6-7 depths distributed from surface to bottom in the water column at the stations on the African shelf and from surface to 200 m at the oceanic stations. Phytoplankton biomass was estimated at 4-6 depths with similar distribution in the water column whereas photophysiological variables (phytoplankton absorption

coefficients and photosynthetic variables) were determined at 3-5 depths within the photic layer. These depths were selected after inspecting the fluorescence profiles.

The spectral light field at sea surface and in the water column was determined at these biological stations with a Licor Li-1800UW following the procedure described by Lorenzo et al. (2004). This approach allows estimation of the transmittance at the air-sea interface and the scalar spectral irradiance at each hour and depth in the water column.

2.2. Nitrate and chlorophyll

Seawater samples for nitrate determinations were preserved frozen at -20º C in polyethylene bottles until their analysis in the shore laboratory. Nitrate concentrations (µM) were determined by segmented flow analysis following the JGOFS recommendations (UNESCO, 1994).

For chl *a*, seawater volumes of 500 ml were filtered through 25 mm Whatman GF/F filters using low vacuum. The filters were frozen at -20 ºC before pigments were extracted on board in 90% acetone for 24 h in the dark at 4 ºC. Chl *a* concentrations (mg m^{-3}) were estimated by fluorometry in a Turner Designs fluorometer calibrated with pure chl *a* (Sigma Chemical). These estimates were also used to calibrate the voltage readings of the Sea Tech fluorometer fitted to the CTD.

2.3. Phytoplankton biomass

Samples of 100 ml preserved in Lugol's iodine were sedimented in composite sedimentation chambers and observed with an inverted microscope to identify and enumerate large phytoplankton (> 20 µm). The smaller species were enumerated from two transects scanned at 400x and 200x, while the whole slide was scanned at 100x to

count the larger species. Phototrophic species of dinoflagellates and ciliates were differentiated following Lessard and Swift (1986) and also using our historical records of epifluorescence microscopy of fresh samples which allow us to distinguish species containing chloroplasts. All organisms with chloroplasts were assumed to be phototrophic. Biovolumes were estimated following Hillebrand et al. (1999) and cell carbon was calculated according to Menden-Deuer and Lessard (2000).

Epifluorescence microscopy was used to identify autotrophic nanoplankton (2-20µm) in samples of 20 ml that were fixed immediately after collection with glutaraldehyde (0.3% final concentration). After 30 min in the dark, these samples were filtered through 0.2 µm black polycarbonate membrane filters placed on top of GF/C backing filters. Excitation with blue light was used to enumerate pigmented nanoplankton that was identified by red autofluorescence. Cell volumes were estimated after taking dimensions and assuming a spherical shape or by approximation to the nearest geometrical shape (Hillebrand et al., 1999). Cell carbon was estimated according to Verity et al. (1992) for autotrophic nanoflagellates and Menden-Deuer and Lessard (2000) for small (<20 µm) naked dinoflagellates.

Prochlorococcus and *Synechococcus* type cyanobacteria and pigmented picoeukaryotes were counted by flow cytometry (FACScalibur flow cytometer) in samples of 4 ml fixed with 2% final concentration of formaldehyde. Samples were run at medium or high speed until 10,000 events were captured. The identification of these 3 groups was done by analysis of multiple bivariate scatter plots of red and orange fluorescence and side scatter. A suspension of yellow-green 1 µm latex beads (Polysciencies, Inc.) was used as internal standard to calculate cell abundances. The bead solution was checked daily through epifluorescence microscopy. *Prochlorococcus* were transformed to biomass assuming a conversion factor of 22 fg C $cell^{-1}$ (Christian

and Karl, 1994; Zubkov et al., 2000), while the factor used to estimate *Synechococcus* biomass was of 250 fg C $cell^{-1}$ (Kana and Gilbert, 1987; Li et al., 1992). Picoeukaryote abundances were converted to biomass using a factor of 2100 fg C $cell^{-1}$ (Campbell et al., 1997).

2.4. Photophysiological variables and primary production

Phytoplankton light absorption coefficients ($a_{ph}(\lambda)$, m^{-1}) were determined according to Arbones et al. (1996). Between 1 and 4 L of seawater were filtered through 25 mm Whatman GF/F filters to determine the optical density spectra (400-750 nm) of concentrated particles at 1 nm bandwidth with a spectrophotometer using a filter moistened with filtered seawater as a blank. The optical density of non-algal material was determined on the same filter after pigment extraction following Kishino et al. (1985). Absorbance at 750 nm was subtracted from all other wavelengths in the spectra before correcting the pathlength amplification according to Arbones et al. (1996).

Photosynthesis-irradiance (P-E) experiments, from which photosynthetic variables were estimated, were carried out in linear incubators refrigerated with thermostatic baths (Arbones et al., 2000). Each incubator housed 14 subsamples collected in 75 ml Corning tissue culture flasks that were inoculated with 3.70 x 10^5 Bq (10 μCi) of $NaH^{14}CO_3$. The bottle at the end of the incubator was covered with aluminium foil for checking dark carbon fixation. After 2 hours of incubation, samples were filtered under low vacuum through 25 mm Whatman GF/F filters which were then exposed to HCl fumes for 12h to eliminate unincorporated inorganic ^{14}C. The incorporated radioactivity (dpm) was estimated in a liquid scintillator counter using the external standard and the channel ratio methods to correct for quenching.

The photosynthetic active radiation (PAR) at each position in the incubator was

checked regularly with a Li-Cor cosine sensor LI-190SA allowing for incident irradiance on the front side of the incubator >1000 µmol quanta m^{-2} s^{-1} for surface samples and <400 µmol quanta m^{-2} s^{-1} for the deepest samples. As the spectral quality of the incident light did not change along these short incubators (Arbones et al., 2000), the spectral irradiance at each position in the incubators $E(\lambda)$ was estimated multiplying the corresponding PAR irradiance by the normalized spectrum of the source tungsten-halogen lamps $E_{NL}(\lambda)$ (Figueiras et al., 1999; Arbones et al., 2000):

$$E_{NL}(\lambda) = E_L(\lambda) / \int_{400}^{700} E_L(\lambda) d\lambda \quad (1)$$

where $E_L(\lambda)$ is the lamp spectrum.

The photosynthetically active radiation absorbed by phytoplankton (E_{PUR}, µmol quanta m^{-3} s^{-1}) at each location in the incubators is:

$$E_{PUR} = \int_{400}^{700} a_{ph}(\lambda) \cdot E(\lambda) d\lambda \quad (2)$$

When photoinhibition was not observed the data were fitted to:

$$P_z^B = P_m^B [1 - exp(-\alpha_{PUR}^B E_{PUR} / P_m^B)] \quad (3)$$

to estimate the light-saturated rate of photosynthesis P_m^B (mg C (mg chl a)$^{-1}$ h^{-1}) and the light-limited slope of the P-E curve α_{PUR}^B (mg C (mg chl a)$^{-1}$ h^{-1} (µmol quanta m^{-3} s^{-1})$^{-1}$) for the light absorbed by phytoplankton. P_z^B (mg C (mg chl a)$^{-1}$ h^{-1}) is the chlorophyll-specific rate of photosynthesis at each sampled depth.

With photoinhibition the data were fitted to:

$$P_z^B = P_s^B[1 - exp(-\alpha_{PUR}^B E_{PUR}/P_s^B)] \cdot exp(-\beta_{PUR}^B E_{PUR}/P_s^B) \quad (4)$$

where P_s^B is the light-saturated rate of photosynthesis in the absence of photoinhibition (mg C (mg chl *a*)$^{-1}$ h^{-1}) and $\beta_{PUR}^B$is the photoinhibition coefficient (mg C (mg chl *a*)$^{-1}$ h^{-1} (µmol quanta m^{-3} s^{-1})$^{-1}$) for the light absorbed by phytoplankton. For these cases with photoinhibition P_m^B was estimated when $\partial P_z^B/\partial E_{PUR} = 0$ (Platt et al. 1980).

The maximum quantum yield for carbon fixation (ϕ_m, mol C fixed (mol quanta absorbed)$^{-1}$) was estimated as:

$$\phi_m = chl\ a\ \alpha_{PUR}^B/43.29 \quad (5)$$

where 43.29 is a factor converting units of α_{PUR}^B: mg of C to moles, µmol quanta to moles and hours to seconds.

The broadband light-limited slope of the P-E curves α^B (mg C (mg chl *a*)$^{-1}$ h^{-1}(µmol quanta m^{-2} s^{-1})$^{-1}$) can be estimated from α_{PUR}^B as:

$$\alpha_{PUR}^B = \alpha^B/\bar{a}_{ph} \quad (6)$$

where $\bar{a}_{ph}$(m^{-1}) is the mean absorption coefficient of phytoplankton weighted by the spectral distribution $E(\lambda)$ of the light in the incubators:

$$\bar{a}_{ph} = \frac{\int_{400}^{700} a_{ph}(\lambda)E(\lambda)d\lambda}{\int_{400}^{700} E(\lambda)d\lambda} \quad (7)$$

The light saturation parameter for photosynthetic active radiation E_k (µmol quanta m^{-2} s^{-1}) is:

$$E_k = P_m^B / \alpha_B \quad (8)$$

Vertical profiles of chl *a* concentration and light absorbed by phytoplankton deduced from hourly spectral light field and phytoplankton absorption coefficients were used in Eqs. (3) and (4) to estimate integrated primary production (PP, g C m^{-2} d^{-1}). Integration was done at hour intervals and 1 m steps from sea surface down to 0.1% surface irradiance.

3. Results and discussion

3.1. Hydrographic variability

The sea surface, as revealed by satellite imagery (Fig. 1), showed the high mesoscale variability that has been repeatedly reported for the region (Barton et al., 1998; Basterretxea and Arístegui, 2000; Sangrà et al., 2009; Benítez-Barrios et al., 2011), where coastal upwelling, filaments and cyclonic and anticyclonic eddies are among the most visible features. Eddies south of the islands were deep and generated by a combined effect of Ekman pumping and topographic perturbation of the mean southward flow of the Canary Current (Arístegui et al., 1994, 1997; Barton et al., 2000; Sangrà et al., 2009; Benítez-Barrios et al., 2011). In contrast, eddies near the upwelling frontal zone were shallower and probably formed by baroclinic instabilities in the upwelling jet (Benítez-Barrios et al., 2011). This difference between the two type of eddies is seen clearly in the vertical profiles of temperature and chlorophyll fluorescence recorded for the long line sampled between the island of La Palma and

Cape Juby on the African coast (Fig. 2a and c). Cyclonic and anticyclonic eddies near La Palma caused vertical excursions of almost 100 m in the thermocline and the deep chlorophyll maximum (DCM). However, vertical displacements were considerably smaller in eddies and filaments near the shelf. Minor uplifts of the thermocline and the DCM were also observed in other filaments (Fig. 2b and d). DCM uplifts caused by cyclones and filaments induced noticeable increases in chl *a* concentration (Fig. 2c and d), a well-known situation for this (Arístegui et al., 1997; Basterretxea et al., 2002) and other regions affected by cyclonic eddies (Falkowski et al., 1991; Vaillancourt et al., 2003; Brown et al., 2008). A much more detailed description of the hydrographic conditions found during this cruise was provided by Barton et al. (2004).

3.2. Clustering stations

In terms of the vertical structure of the water column, the biological stations could be clustered into three groups that can be ranked according to an oligotrophic – eutrophic gradient (Fig. 3). The first group is formed by oligotrophic stations, in both open ocean and anticyclonic eddies (O&A, Fig. 3a). These stations showed very low nitrate levels in the stratified upper layer and a well-developed DCM located at a depth (78 ± 21 m) that was not significantly different ($P = 0.2$, t-test for two samples, n = 7) from the depth of the 1% of surface irradiance (91 ± 14 m). The second group includes transitional stations associated with filaments and cyclonic eddies (F&C, Fig. 3b). In this group nitrate was not totally depleted in the photic layer and the mean depth of the DCM (44 ± 14 m) was significantly shallower ($P < 0.001$, t-test for two samples, n = 20) than the mean depth of 1% of surface irradiance (66 ± 17 m). The third group comprises 4 shelf stations that were affected by upwelling (Upw, Fig. 3c). There was no well-defined DCM or subsurface chlorophyll maximum at these stations, instead chl *a*

was spread in the upper mixed layer, always within the photic zone. The locations of all these stations belonging to the three groups are given in Fig. 1, where a coastal (eutrophic) – ocean (oligotrophic) gradient is evident, though one transitional station is found in the oligotrophic zone and two oligotrophic stations are situated in the transitional area.

Phytoplankton size-biomass distribution supports this grouping of stations (Fig. 4) following the identified coastal – ocean gradient. This is a gradient consistent with the classical view of dominance of small cells in stratified and nutrient-poor surface oceanic waters and dominance of large phytoplankton in nutrient-rich coastal waters (Ryther, 1969; Cushing, 1989), which has been reported for other coastal upwelling systems (Lorenzo et al., 2005). Thus, the low phytoplankton biomass with dominance of small forms (picophytoplankton representing 76 ± 8% and pico- plus nanophytoplankton accounting for 90 ± 4% of total phytoplankton biomass) that was measured in oligotrophic and anticyclonic stations (Fig. 4a) contrasts with the high phytoplankton biomass and dominance of large size classes (microphytoplankton accounting for 79 ± 6% of total phytoplankton biomass) recorded in shelf stations affected by upwelling (Fig. 4d). In between we found transitional stations with high variability in phytoplankton size-biomass distribution. In this group there were stations with dominance of nano- and microphytoplankton (Fig. 4b) and stations with evident hegemony of picophytoplankton (Fig. 4c). It has been suggested that the high level of mesoscale activity that commonly occurs in this transitional zone, where oligotrophic and upwelled waters meet, strongly modulates the patterns of phytoplankton biomass distribution and the community size-structure (Baltar et al., 2009; Anabalón et al., 2014).

3.3. Photosynthetic performance

Photosynthetic variables in the three groups of stations showed vertical profiles (Fig. 5) in which maximum carbon fixation rates (P_m^B) and light saturation parameters (E_k) decreased with depth while maximum quantum yields (ϕ_m) increased with depth. However, the increase of ϕ_m with depth was not so evident at upwelling stations (Fig. 5c), probably because nutrient limitation at the surface was not as severe as in the two other groups of stations (Fig. 3). This resulted in relatively high ϕ_m values at the surface in upwelling stations. Low ϕ_m values in surface waters of stratified oligotrophic seas, like those shown in Fig. 5a, may be caused not only by the presence of a high fraction of non-photosynthetic pigments (photoprotective pigments) that do not channel the light absorbed by phytoplankton to photosynthesis, but also they can result from nutrient limitation induced by the low nutrient levels present in these environments (Babin et al. 1996; Lorenzo et al., 2004). In this respect it is to be noted that maximum quantum yields in the lower part of the photic layer (below $0.5Z_{eu}$) were near the maximum value of 0.08 mol C fixed (mol quanta absorbed)$^{-1}$ expected for environmental conditions with high nutrient concentrations (Lindley et al., 1995). The pattern depicted in Fig. 5a, b for oligotrophic and transitional stations, with higher P_m^B and $E_k$values at the surface and higher ϕ_m values at the bottom of the photic layer, is usually found in stratified oligotrophic seas (Lorenzo et al., 2004) and has been interpreted as photoacclimation of phytoplankton to the irradiance field in a water column with enhanced nutrient availability at the bottom of the photic layer (Falkowski et al., 1980; Cullen et al., 1992).

Although we did not find any clear relationship between photosynthetic variables and phytoplankton size-structure, clear signals of photoadaptation and/or photoacclimation were revealed when photosynthetic variables were ordered according to the depth of the

photic zone (Table 1; Fig. 6). At the surface there were differences in the four variables, with oligotrophic stations exhibiting lower ϕ_m, α^B and P_m^B and higher E_k values than the other two groups (Table 1, Fig. 6a). At the other two depths differences basically occurred in P_m^B, with oligotrophic stations displaying in general lower values; the exception was seen at the bottom of the photic layer where oligotrophic and filament stations had similar photosynthetic variables (Table 1; Fig 6b,c). These P-E curves (Table 1; Fig. 6) are quite similar to the curves derived by Uitz et al. (2008) for micro-, nano- and picophytoplankton using a larger data set. Specifically the curve that these authors derived for picophytoplankton is very similar to the curve obtained here for oligotrophic waters at sea surface, where picophytoplankton dominated in the phytoplankton community.

3.4. Primary production: significance of the DCM in the oligotrophic environment

Integrated primary production (PP) showed a coastal-ocean gradient similar to that depicted by integrated chl *a* (Table 2), which is characterised by high values at the coastal stations and lowest values at the oligotrophic stations. PP varied between 3.8 g C m^{-2} d^{-1} measured in the upwelling zone and 0.24 g C m^{-2} d^{-1} determined in the oligotrophic environment; a range of values that has been reported for this (Morel et al., 1996; Basterretxea and Arístegui, 2000) and other eastern boundary upwelling regions (Piskaln et al., 1996; Montecino et al., 2004; Lorenzo et al., 2005).

Integrated PP and integrated chl *a* were strongly correlated (Fig. 7), which is not surprising because PP was estimated after including chl *a* in Eqs. (3) and (4). However, this correlation is not used here as an empirical relationship, instead it is used to explore which variables have the highest influence on primary production along this coastal-ocean (eutrophic-oligotrophic) gradient. Thus, it can be seen that the correlation

between PP and integrated chl *a* dropped from significant values in the upwelling to insignificant in the oligotrophic stations (Fig. 7). This suggests that in this environment some factor other than chlorophyll (phytoplankton biomass) was decisive for PP. Variations in PP were directly linked in this oligotrophic environment to those in carbon fixation at the DCM (Fig. 8a), which occupied a depth interval responsible for 36% of PP and where integrated primary production and integrated chl *a* concentration were not correlated ($r^2 = 0.1$, $P = 0.49$; $n = 7$); defining the DCM as the layer that showed a steady increase-decrease in chl *a* concentration above and below of the maximum chl *a* value of the water column. However, PP at these oligotrophic stations was negatively related to the depth of the 1% surface light level (Fig. 8b), a type of relationship that has been previously reported for stratified waters in the Atlantic Ocean (Herbland and Voituriez, 1979) where the depth of the DCM and the depth of the nitracline coincide (Herbland and Voituriez, 1979; Lorenzo et al., 2004). Considering these two relationships (Fig. 8a, b) and that the DCM and the 1% light level were located at roughly the same depth (Fig. 3a), it can be inferred that light availability was the main factor controlling PP in this oligotrophic environment. According to the relationship in Fig. 8b, a downward displacement of 20 m in a DCM situated at 70 m causes a decrease of 25% in PP. The decrease in PP will be 34% for a DCM located at 90 m. The corresponding decreases in PP for downward displacements of 50 m in a DCM located at 70 m and 90 m will be of 63% and 85%, respectively.

The reason for this strong influence of light on carbon fixation at the DCM of oligotrophic stations is that photosynthesis at these depths occurred at light levels near the light saturation parameter of the P-E relationships (Fig. 9a). Consequently, a slight decrease in the light received by phytoplankton, caused by a downward displacement of the DCM, induces a substantial decrease in carbon fixation because of the high slope of

the P-E relationships. Maximum quantum yields of carbon fixation recorded at the bottom of the photic layer in oligotrophic stations were close to the maximum possible value (Table 1), indicating that the slope of the P-E relationships was the highest possible for phytoplankton inhabiting this environment. In contrast, an increase in the light received by phytoplankton due to an upward displacement of the DCM, should not have such high influence on chl *a* specific carbon fixation, because once the maximum photosynthetic rate is achieved further increases in irradiance have no effect on PP. In this case, increases in chl *a* specific carbon fixation should take place by photoacclimation or through shifts to phytoplankton communities with higher maximum photosynthetic rates, which are two processes that require time.

At the stations belonging to the other two groups (F&C and Upw), the range of the light intensity received by phytoplankton in the layer with maximum chl *a* concentration was greater and reached the region of maximum photosynthetic rate (Fig. 9b,c). Moreover, in contrast to what happened in the O&A stations, carbon fixation at the depth of 1% of light in F&C and Upw stations was a minor part of the total integrated PP. Because of this, PP and integrated chl *a* at these stations were correlated (Fig. 7) while irradiance had negligible influence on carbon fixation. The similarity of the photosynthetic variables recorded at the Z_{eu} of both O&A and F&C stations (Table 1), suggests that initial increases in PP in filament and cyclones as response to water uplifts should occur through an increase in phytoplankton chlorophyll. This increase is favoured by the absence of light limitation of the photosynthetic response (Fig. 9b) under non nutrient-limiting conditions (Fig. 3b). Later, photoacclimation and/or photoadaptation processes could lead to changes in photosynthetic variables (Table 1) and so induce additional PP increases.

These results show that, as expected, eddies induced considerable vertical displacements of the DCM in the Canary region. They also show that these vertical movements of the DCM should be taken into account when estimating and/or modelling primary production in the oligotrophic ocean because variations in the light received by phytoplankton cause significant increases and decreases in primary production. As the Canary region is an important eddy generation zone in which anticyclones dominate over cyclones (Sangrà et al., 2009), primary production can be significantly reduced, at least in the core of the eddies, where downwelling lowers the DCM to depths below light saturation levels for photosynthesis.

Acknowledgements

We thank the officers and crew of the BIO 'Hesperides' and the members of the UTM (CSIC) who participated in the cruise. This work was funded by the EU project CANIGO (MAS3.CT96-0060). JA and MFM were partly supported by projects HOTMIX (CTM2011-30010-C02/MAR) and PUMP (CTM2012-33355), which also partly supported EDB.

References

Anabalón, V., Arístegui, J., Morales, C.E., Andrade, I., Benavides, M., Correa-Ramírez, M.A., Espino, M., Ettahiri, O., Hormazabal, S., Makaoui, A., Montero, M.F., Orbi, A., 2014. The structure of planktonic communities under variable coastal upwelling conditions off Cape Ghir (31 ºN) in the Canary Current System (NW Africa). Prog. Oceanogr. 120, 320-339.

Arbones, B., Figueiras, F.G., Varela, R., 2000. Action spectrum and maximum quantum yield of carbon fixation in natural phytoplankton populations: implications for primary production estimates in the ocean. J. Mar. Syst. 26, 97-114.

Arbones, B., Figueiras, F.G., Zapata, M., 1996. Determination of phytoplankton absorption coefficient in natural seawater samples: evidence of a unique equation to correct the pathlength amplification on glass-fiber filters. Mar. Ecol. Prog. Ser. 137, 293-304.

Arístegui, J., Barton, E.D., Tett, P., Montero, M.F., García-Muñoz, G., Basterretxea, G., Cussatlegras, A.S., Ojeda, A., de Armas, D., 2004. Variability in plankton community structure, metabolism, and vertical carbon fluxes along an upwelling filament (Cape Juby, NW Africa). Prog. Oceanogr. 62, 95-113.

Arístegui, J., Sangrà, P., Hernández-León, S., Cantón, M., Hernández-Guerra, A., Kerling, J.L., 1994. Island-induced eddies in the Canary Islands. Deep-Sea Res. I 41, 1509-1525.

Arístegui, J., Tett, P., Hernández-Guerra, A., Basterretxea, G., Montero. M.F., Wild, K., Sangrá. P., Hernández-León, S., Cantón, M., García-Braun, J.A., Pacheco, M., Barton, E.D., 1997. The influence of island-generated eddies on chlorophyll distribution: a study of mesoscale variation around Gran Canaria. Deep-Sea Res. I 44, 71-96.

Babin, M., Morel, A., Claustre, H., Bricaud, A., Kolber, Z., Falkowski, P.G., 1996. Nitrogen and irradiance dependent variations of maximum quantum yield of carbon fixation in eutrophic, mesotrophic and oligotrophic marine systems. Deep-Sea Res. I 43, 1241-1272.

Baltar, F., Arístegui, J., Montero, M.F., Espino, M., Gasol, J.M., Herdndl, G.J., 2009. Mesoscale variability modulates seasonal changes in the trophic structure of nano- and picoplankton communities across the NW Africa-Canary Islands transition zone. Prog. Oceanogr. 83, 180-188.

Barton, E.D., Basterretxea, G., Flament, P., Mitchelson-Jacob, E.G., Jones. B., Arístegui, J., Herrera, F., 2000. Lee region of Gran Canaria. J. Geophys. Res. 105 (C7), 17173-17193.

Barton, E.D., Arístegui, J., Tett, P., Cantón, M., García-Braun, J., Hernández-León, S., Nykjaerf, L., Almeida, C., Almunia, J., Ballesteros, S., Basterretxea, G., Escánez, J., García-Weill, L., Hernández-Guerra, A., López-Laatzen, F., Molina, R., Montero, M.F., Navarro-Pérez, E., Rodríguez, J.M., van Lenning, K., Vélez, H., Wild, K., 1998. The transition zone of the Canary Current upwelling region. Prog. Oceanogr. 41, 455-504.

Barton, E.D., Arístegui, J., Tett, P., Navarro-Pérez, E., 2004. Variability in the Canary Islands area of filament-eddy exchanges. Prog. Oceanogr. 62, 71-94.

Basterretxea, G., Arístegui, J., 2000. Mesoscale variability in phytoplankton biomass distribution and photosynthetic parameters in the Cabary-NW African coastal transition zone. Mar. Ecol. Prog. Ser. 197, 27-40.

Basterretxea, G., Barton, E.D., Tett, P., Sangrà, P., Navarro-Pérez, E., Arístegui, J., 2002. Eddy and deep chlorophyll maximum response to wind-shear in the lee of Gran Canaria. Deep-Sea Res. I 49, 1087-1101.

Benítez-Barrios, V.M., Pelegrí, J.L., Hernández-Guerra, A., , Lwiza, K.M.M., Gomis, D., Vélez-Belchí, P., Hernández-León, S., 2011. Three-dimensional circulation in the NW Africa costal transition zone. Prog. Oceanogr. 91, 516-533.

Brown, S.L., Landry, M.R., Selph, K.E., Yang, E.J., Rii, Y, M., Bidigare, R.R., 2008. Diatoms in the desert: Plankton community response to a mesoscale eddy in the subtropical North Pacific. Deep-Sea Res. II 55, 1321-1333.

Campell, L., Liu, H., Nolla, H.A., Vaulot, D., 1997. Annual variability of phytoplankton and bacteria in the subtropical North Pacific Ocean at Station ALOHA during the 1991-1994 ENSO event. Deep-Sea Res. I 44, 167-192.

Christian, J.R., Karl, D.M., 1994. Microbial community structure at the US-Joint Global Ocean Flux Study Station ALOHA: Inverse methods for estimating biochemical indicator ratios. J. Geophys. Res. 99, 14269-14276.

Cullen, J.J., 2015. Subsurface chlorophyll maximum layers: enduring enigma or mystery solved? Annu. Rev. Mar. Sci. 7, 207-239.

Cullen, J.J., Lewis, M.R., Davis, C.O., Braber, R.T., 1992. Photosynthetic characteristics and estimated growth rates indicate grazing is the proximate control of primary production in the equatorial Pacific. J. Geophys. Res. 97, 639-654.

Cushing, D.H., 1989. A difference in structure between ecosystems in strongly stratified waters and in those that are only weakly stratified. J. Plankton Res. 11, 1-13.

Falkowski, P.G., 1980. Light-shade adaptation in marine phytoplankton. In: Falkowski, P.G. (Ed.), Primary productivity in the sea. Plenum, New York, pp. 99-120.

Falkowski, P.G., Ziemann, D., Kolber, Z., Bienfang, P.K., 1991. Role of eddy pumping in enhancing primary production in the ocean. Nature 352, 55-58.

Figueiras, F.G., Arbones, B., Estrada, M., 1999. Implications of bio-optical modelling of phytoplankton in Antarctic waters: further evidence of no light limitation in the Bransfield Stait. Limnol. Oceanogr. 44, 1599-1608.

Herbland, A., Voituriez, B., 1979. Hydrological structure analysis for estimating the primary production in the tropical Atlantic Ocean. J. Mar. Res. 37, 87-101.

Hillebrand, H., Dürselen, C., Kirschtel, D., Pollingher, U., Zohary, T., 1999. Biovolume calculation for pelagic and benthic microalgae. J. Phycol. 35, 403-424.

Joint, I., Inall, M., Torres, R., Figueiras, F.G., Álvarez-Salgado, X. A., Rees, A. P., Woodward, E.M.S., 2001. Two lagrangian experiments in the Iberian Upwelling System: tracking an upwelling event and an off-shore filament. Prog. Oceanogr. 51, 221-248.

Kana, T., Gilbert, P.M., 1987. Effects of irradiances up to 2000 μm E m^{-2} s^{-1} on marine Synechococcus WH 7803-I. Growth, pigmentation, and cell composition. Deep-Sea Res. I 34, 479-516.

Kishino, M., Takahashi, N., Olami, N., Ichimura, S., 1985. Estimation of the spectral absorption coefficients of phytoplankton in the sea. Bull. Mar. Sci. 37, 634-642.

Lessard, E.J., Swift, E., 1986. Dinoflagellates from the North Atlantic classified as phototrophic or heterotrophic by epifluorescence microscopy. J. Plankton Res. 8, 1209-1215.

Li, W.K.W., Dickie, P.M., Irwin, B.D., Wood, A.M., 1992. Biomass of bacteria, cyanobacteria, prochlorophytes and photosynthetic eukaryotes in the Sargasso Sea, Deep-Sea Res. I 39, 501-519.

Lindley, S.T., Bidigare, R.R., Barber, R.T., 1995. Phytoplankton photosynthesis parameters along 140ºW in the equatorial Pacific. Deep-Sea Res. II 42, 441-463.

Lorenzo, L. M., Figueiras, F.G., Tilstone, G.H., Arbones, B., Mirón, I., 2004. Photosynthesis and light regime in the Azores Front region during summer: are light-saturated computations of primary production sufficient? Deep-Sea Res. I 51, 1229-1244.

Lorenzo, L.M., Arbones, B., Tilstone, G.H., Figueiras, F.G., 2005. Across-shelf variability of phytoplankton composition, photosynthetic parameters and primary production in the NW Iberian upwelling system. J. Mar. Syst. 54, 157-173.

McAndrew, P.M., Bidigare, R.R., Karl, D.M., 2008. Primary production and implications for metabolic balance in Hawaiian lee eddies. Deep-Sea Res. II 55, 1300-1309.

McGillicuddy, D.J., Robinson, A.R., Siegel, D.A., Jannasch, H.W., Johnson, R., Dickey, T.D., McNeil, J., Michaels, A.F., Knap, A.H., 1998. Influence of mesoscale eddies om new production in the Sargasso Sea. Nature 394, 263-266.

Menden-Deuer, S., Lessard, E.J., 2000. Carbon to volume relationships for dinoflagellates, diatoms, and other protist plankton. Limnol. Oceanogr. 45, 569-579.

Montecino, V., Astoreca, R., Alarcón, G., Retamal, L., Pizarro, G., 2004. Bio-optical characteristics and primary productivity during upwelling and non-upwelling conditions in a highly productive coastal ecosystem off central Chile (~36ºS). Deep-Sea Res. II 51, 2413-2426.

Morel, A., Antoine, D., Babin, M., Dandonneau, Y., 1996. Measured and modeled primary production in the northeast Atlantic (EUMELI JGOFS program): The impact of natural variations in photosynthetic parameters on model predictive skill. Deep-Sea Res. I 43, 1273-1304.

Piedeleu, M., Sangrà, P., Sánchez-Vidal, A., Fabrés, J., Gordo, C., Calafat, A., 2009. An observational study of oceanic eddy generation mechanisms by tall deep-waters

islands (Gran Canaria). Geophys. Res. Lett. 36, L14605, doi:10.1029/2008GL037010.

Pilskaln, C.H., Paduan, J.B., Chavez, F.P., Anderson, R.Y., Berelson, WM., 1996. Carbon export and regeneration in the coastal upwelling system of Monterey Bay, central California. J. Mar. Res. 54, 1149-1178.

Pingree, R.D., Pugh, P.R., Holligan, P.M., Forster, G.R., 1975. Summer phytoplankton blooms and red tides along tidal fronts in the approaches to the English Channel. Nature 258, 672-677.

Platt, T., Gallegos, C.L., Harrison, W.G., 1980. Photoinhibition of photosynthesis in natural assemblages of marine phytoplankton. J. Mar. Res. 38, 687-701.

Rodríguez, J.M., Hernández-León, S., Barton, E.D., 1999. Mesoscale distribution of fish larvae in relation to an upwelling filament off Northwest Africa. Deep-Sea Res. I 46, 1969-1984.

Ryther, J.H., 1969. Photosynthesis and fish production in the sea. Science 166,72-76.

Sangrà, P., Auladell, M., Marrero-Díaz, A., Pelegrí, J.L., Fraile-Nuez, E., Rodríguez-Santana, A., Martín, J.M., Mason, E., Hernández-Guerra, A., 2007. On the nature of oceanic eddies shed by the island of Gran Canaria. Deep-Sea Res. I 54, 687-709.

Sangrà, P., Pelegrí, J.L., Hernández-Guerra, A., Arregui, I., Martín, J.M., Marrero-Díaz, A., Martínez, A.W., Ratsimandresy, A., Rodríguez-Santana, A. 2005. Life history of an anticyclonic eddy. J. Geophys. Res. 11, C03021.

Sangrà, P:, Pascual, A., Rodríguez-Santana, A., Machín, F., Mason, E., McWillians, J.C., Pelegrí, J.L., Dong, C., Rubio, A., Arístegui, J., Marrero-Díaz, A., Hernández-Guerra, A., Martínez-Marrero, A., Auladell, M., 2009. The Canary Eddy Corridor: A major pathway for long-lived eddies in the subtropical North Atlantic. Deep-Sea Res. I 56, 2100-2114.

UNESCO. 1994. Protocols for the Joint Global Ocean Flux Study (JGOFS) Core Measurement. Intergovernmental Oceanographic Commission, Manual and Guides 29, p. 169.

Vaillancourt, R.D., Marra, J., Seki, M.P., Parsons, M.L., Bidigare, R.R., 2003. Impact of a cyclonic eddy on phytoplankton community structure and photosynthetic competency in the subtropical North Pacific Ocean. Deep-Sea Res. I 50, 829-847.

Verity, P.G., Robertson, C.Y., Tronzo, C.R., Andrews, M.G., Nelson, J.R., Sieracki, M.E., 1992. Relationships between cell volume and the carbon and nitrogen content of marine photosynthetic nanoplankton. Limnol. Oceanogr. 37, 357-366.

Zubkov, M.V., Sleigh, M.A., Burkill, P.H., 2000. Assaying picoplankton distribution by flow cytometry of underway samples collected along a meridional transect across the Atlantic Ocean. Aquat. Microb. Ecol. 21, 13-20.

Table 1. Average (± SE) values of the photosynthetic variables (P_m^B, α^B, E_k, and ϕ_m) determined at three depths within the photic layer (surface; 0.5Zeu, middle of the photic layer and Zeu, bottom of the photic layer) for the three groups of stations identified in the sampled region (O&A, oligotrophic stations; F&C, transitional stations; Upw, upwelling stations).

Depth	Group	P_m^B	α^B	E_k	ϕ_m
Surface	O&A (n = 2)	3.87 ± 0.73	0.008 ± 0.001	488 ± 37	0.017 ± 0.0002
	F&C (n = 6)	5.33 ± 0.86	0.017 ± 0.002	325 ± 48	0.031 ± 0.002
	Upw (n = 4)	4.51 ± 1.10	0.021 ± 0.003	216 ± 39	0.054 ± 0.008
0.5Zeu	O&A (n= 6)	2.09 ± 0.41	0.028 ± 0.006	93 ± 26	0.062 ± 0.020
	F&C (n = 5)	3.31 ± 0.90	0.023 ± 0.001	147 ± 40	0.031 ± 0.005
	Upw (n = 4)	3.29 ± 0.65	0.027 ± 0.008	169 ± 27	0.055 ± 0.010
Zeu	O&A (n = 5)	1.29 ± 0.29	0.038 ± 0.010	38 ± 8	0.064 ± 0.018
	F&C (n = 4)	1.23 ± 0.23	0.041 ± 0.010	35 ± 7	0.083 ± 0.020
	Upw (n = 3)	2.00 ± 0.08	0.026 ± 0.005	84 ± 21	0.057 ± 0.010

Table 2. Average (± SD) primary production (PP, g C m^{-2} d^{-1}) and chlorophyll *a* (chl *a*) concentration (mg m^{-2}) integrated over the photic layer (defined as de layer above the depth of 0.1% of surface irradiance) determined for the three groups of stations identified in the sampled region (O&A, oligotrophic stations; F&C, transitional stations; Upw, upwelling stations).

Group	PP	chl *a*
O&A (n = 7)	0.36 ± 0.11	37 ± 4
F&C (n = 20)	0.82 ± 0.31	50 ± 17
Upw (n = 4)	2.50 ± 1.21	112 ± 36

Figure captions

Fig. 1. Sea Surface AVHRR temperature image of 24 August 1999 for the Canary Island region showing several cyclonic (C) and anticyclonic (A) eddies and two filaments (F) near Cape Juby on the African coast. The eddy field evolved continuously during the sampling period 5-27 August so that individual stations do not necessarily correspond to features seen in the image. The stations sampled (black dots) and clusters discussed in the text for the biological stations are also shown. Red squares highlight oligotrophic and anticyclonic (O&A) stations, blue circles correspond to filament and cyclonic (F&C) stations and green triangles are upwelling (Upw) stations. The two lines (blue and red) denote the two sections (long and short) depicted in figure 2.

Fig. 2. (a) Vertical distribution of temperature (ºC) for a long section from Cape Juby to northwest of the island of La Palma and (b) for a shorter section from Cape Juby to Fuerteventura (see Fig. 1). Vertical distributions of chlorophyll *a* (Chl *a*) concentration (mg m^{-3}) for the two sections are also given (c, d). Cyclones (C), anticyclones (A) and filaments (F) are identified on the top of panels (a) and (b). See figure 1 for the location of the two sections.

Fig. 3. Mean (± SE) vertical profiles of temperature (ºC), chlorophyll *a* concentration (Chl *a* fluorescence) and nitrate concentration (NO_3^-) for the three groups of stations identified in the sampled region. (a) Oligotrophic and anticyclonic (O&A) stations, (b) filament and cyclonic (F&C) stations and (c) upwelling (Upw) stations. Average depth of the 1% and 0.1% of surface irradiance are denoted by horizontal continuous and dashed lines, respectively. See text for more details.

Fig. 4. Representative vertical profiles of size-fractionated phytoplankton biomass for (a) oligotrophic and anticyclonic (O&A) stations, (b and c) filament and cyclonic (F&C) stations and (d) upwelling (Upw) stations. Horizontal continuous line denotes the depth of the deep chlorophyll maximum (DCM). See text for more details.

Fig. 5. Mean (± SE) vertical profiles for maximum photosynthetic rate P_m^B (brown circles), light saturation parameter for PAR irradiance E_k (green squares) and maximum quantum yield ϕ_m (blue triangles) for (a) oligotrophic and anticyclonic (O&A) stations, (b) filament and cyclonic (F&C) stations and (c) upwelling (Upw) stations. Horizontal continuous and dashed lines denote the average middle depth of the photic layer ($0.5Z_{eu}$) and the average depth of the bottom of the photic layer (Z_{eu}), respectively.

Fig. 6. Mean photosynthesis-irradiance relationships at three depths (a) surface, (b) middle depth of the photic layer $0.5Z_{eu}$ and (c) depth of the bottom of the photic layer Z_{eu} for each of the three clusters of stations identified: (O&A) oligotrophic and anticyclonic stations, (F&C) filament and cyclonic stations and (Upw) upwelling stations. The mean values (±SE) of the corresponding photosynthetic variables are given in Table 1.

Fig. 7. Relationship between integrated chlorophyll a (chl *a*) and integrated primary production (PP) over the photic layer. Partial determination coefficients are given for each of the three clusters of stations identified: (O&A) oligotrophic and anticyclonic stations, (F&C) filament and cyclonic stations and (Upw) upwelling stations.

Fig. 8. (a) Relationship between primary production at the DCM and integrated primary production over the photic layer and (b) relationship between the depth of the photic layer and integrated primary production over the photic layer at the stations belonging to the oligotrophic and anticyclonic (O&A) cluster. In (a) the DCM was defined as the layer showing a steady increase-decrease in chl *a* concentration above and below of the maximum chl *a* value in the water column.

Fig. 9. Mean (± SE) photosynthesis-irradiance curves (a) at the DCM of oligotrophic and anticyclonic (O&A) stations, (b) at the DCM of filament and cyclonic (F&C) stations and (c) at surface (continuous line) and bottom of the photic layer (dashed line) of upwelling (Upw) stations. In (c) the vertical dashed-dotted line denotes the position of the light saturation parameter E_k for the photosynthesis-irradiance curve at the bottom of the photic layer.

Figure(s)
Click here to download Figure(s): Fig 1.docx

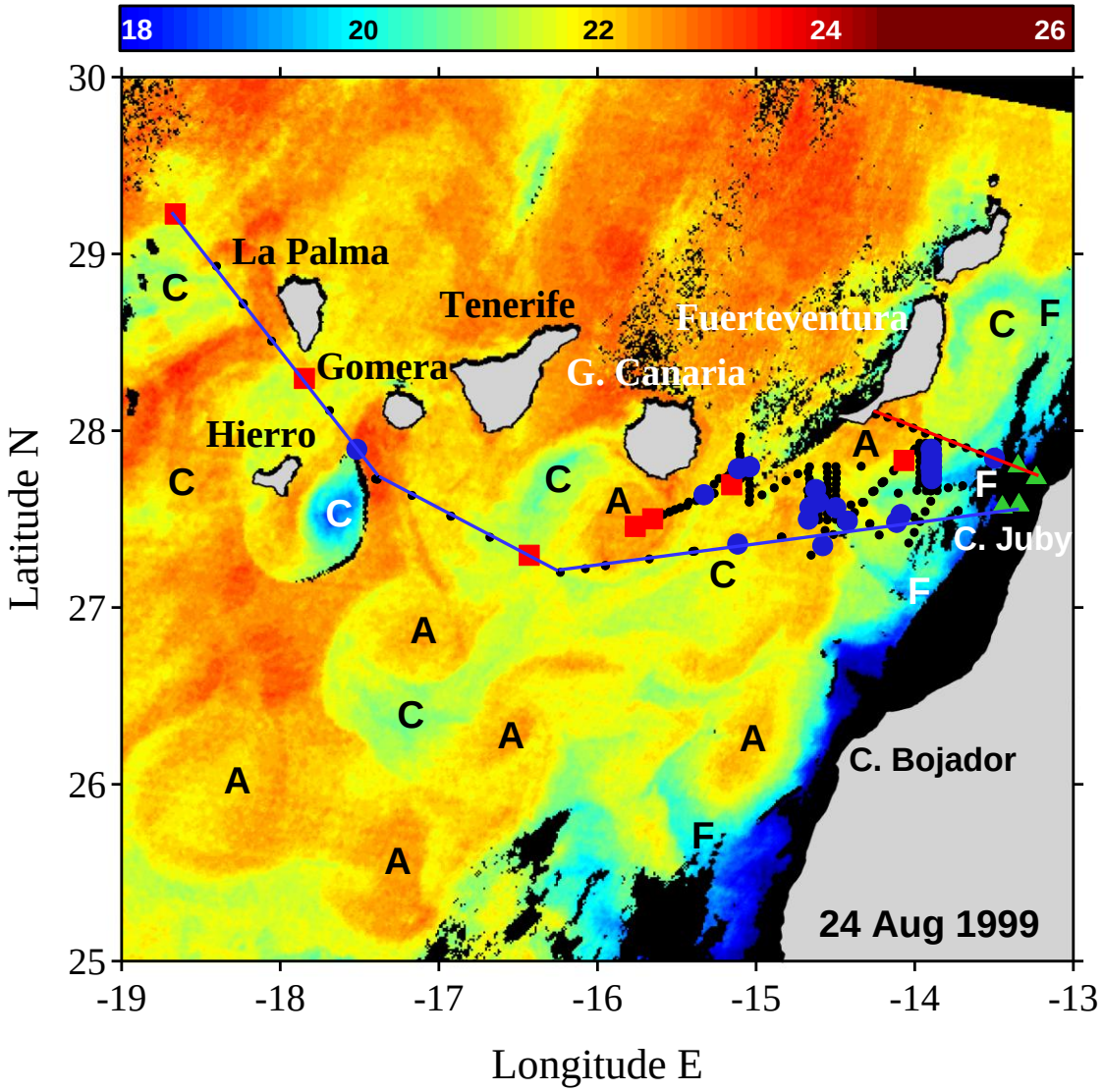

Fig. 1
Figueiras et al.

Figure(s)

Click here to download Figure(s): Fig 2.docx

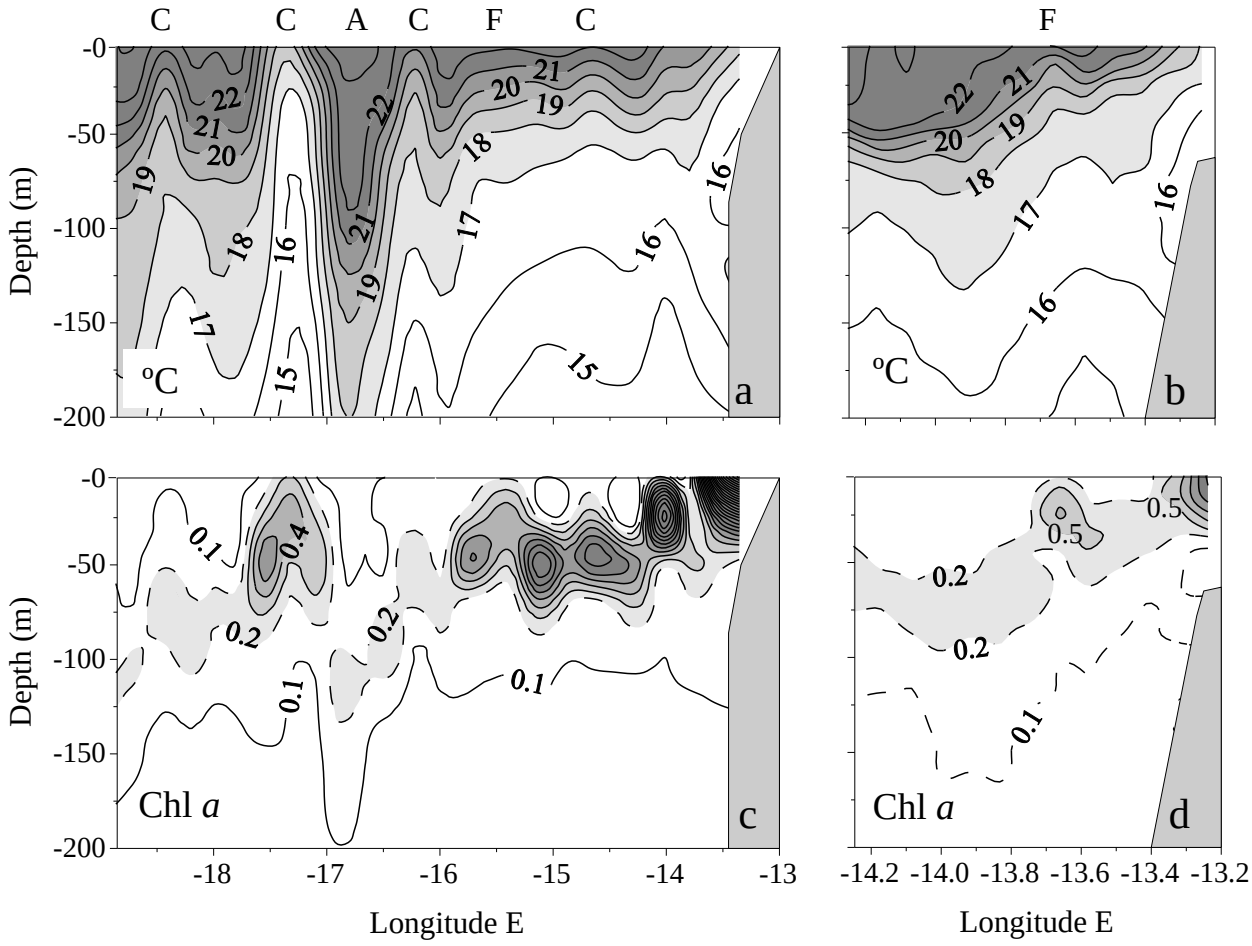

Fig. 2
Figueiras et al.

Figure(s)

Click here to download Figure(s): Fig 3.docx

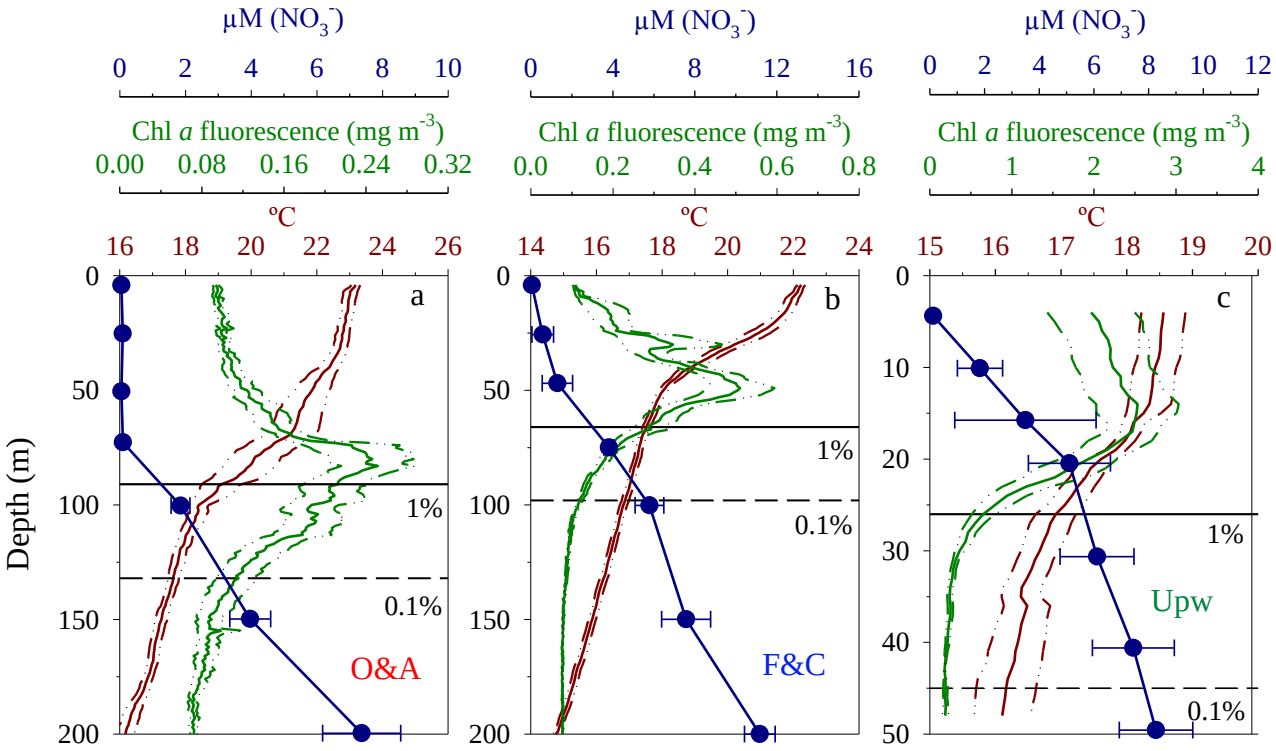

Fig. 3
Figueiras et al.

Figure(s)

Click here to download Figure(s): Fig 4.docx

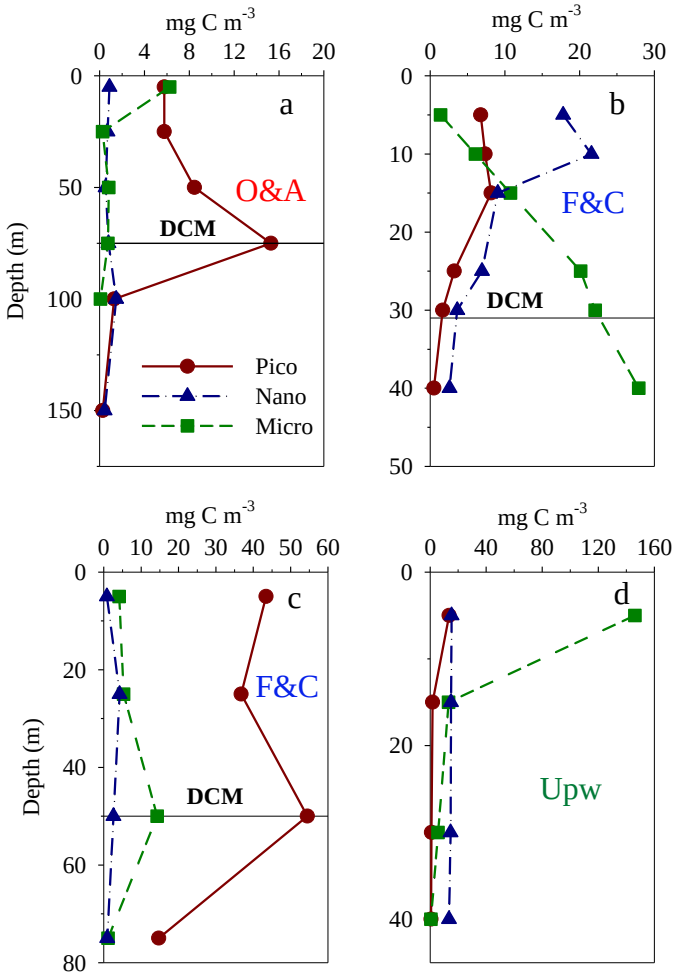

Fig. 4
Figueiras et al.

Figure(s)

Click here to download Figure(s): Fig 5.docx

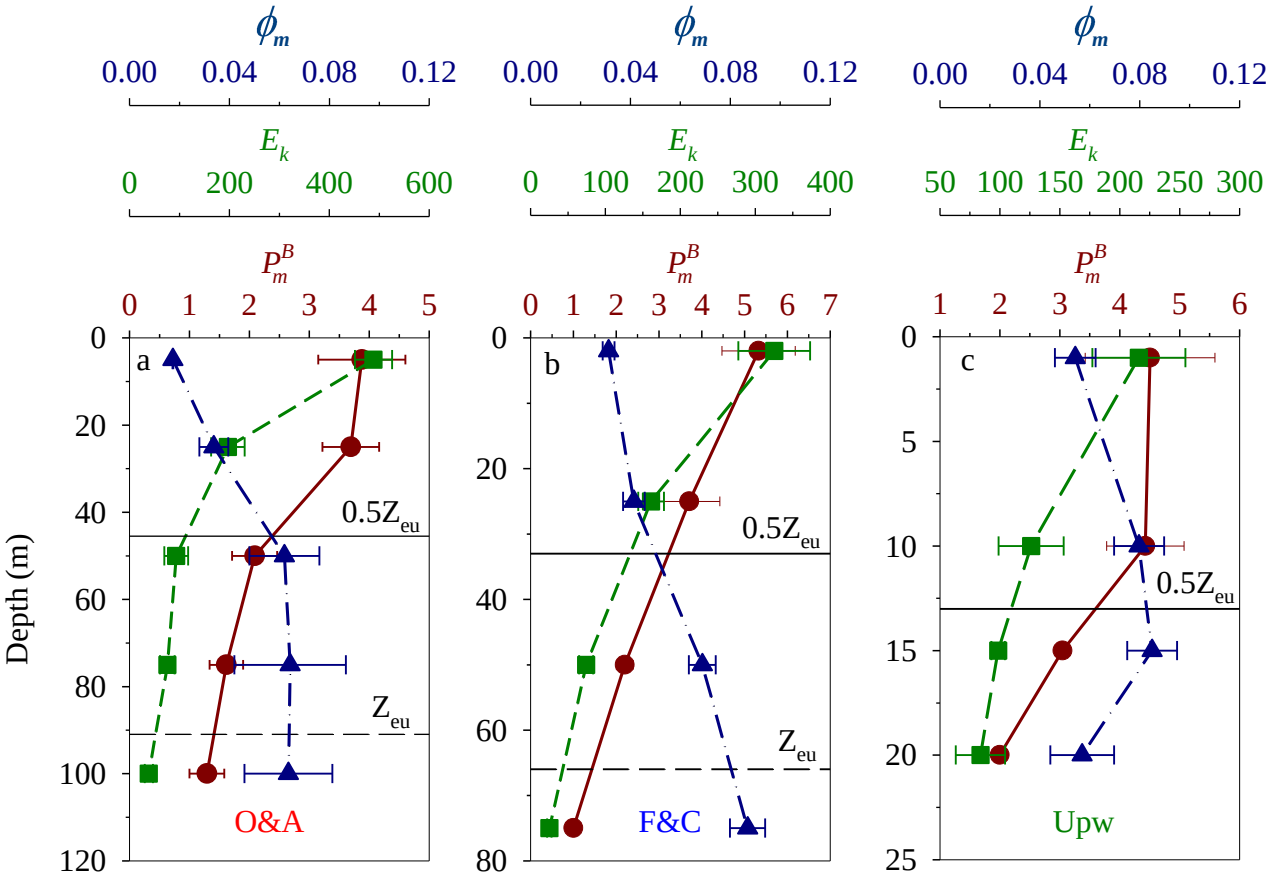

Fig. 5
Figueiras et al.

Figure(s)
Click here to download Figure(s): Fig 6.docx

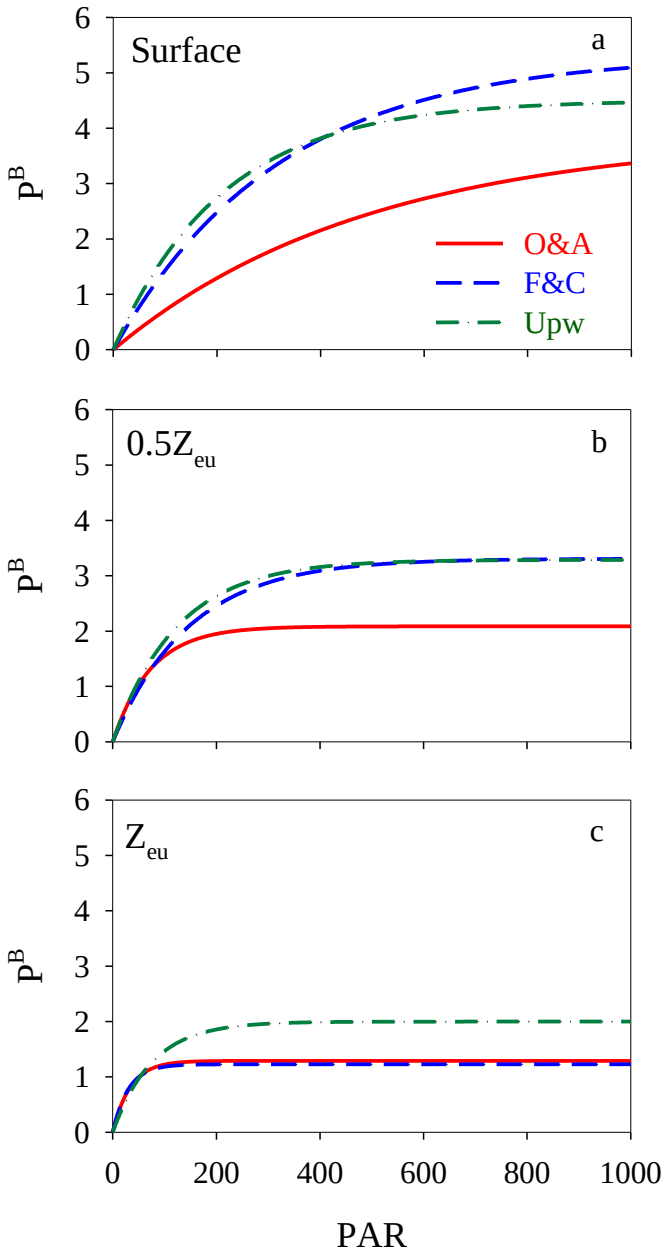

Fig. 6
Figueiras et al.

Figure(s)

Click here to download Figure(s): Fig 7.docx

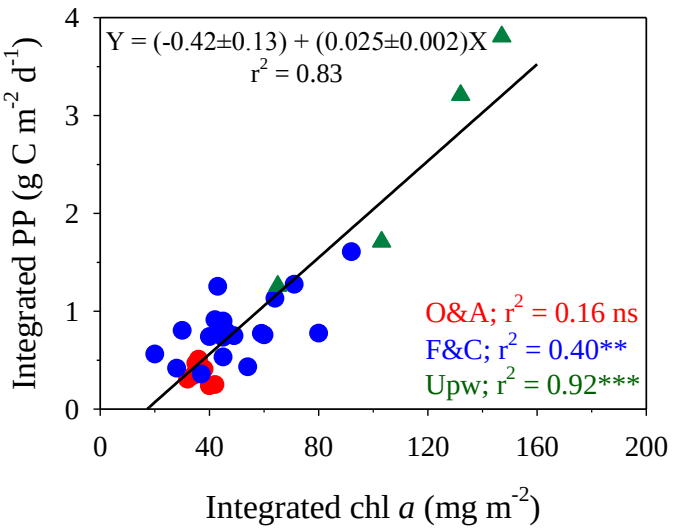

Fig. 7
Figueiras et al.

Figure(s)
Click here to download Figure(s): Fig 8.docx

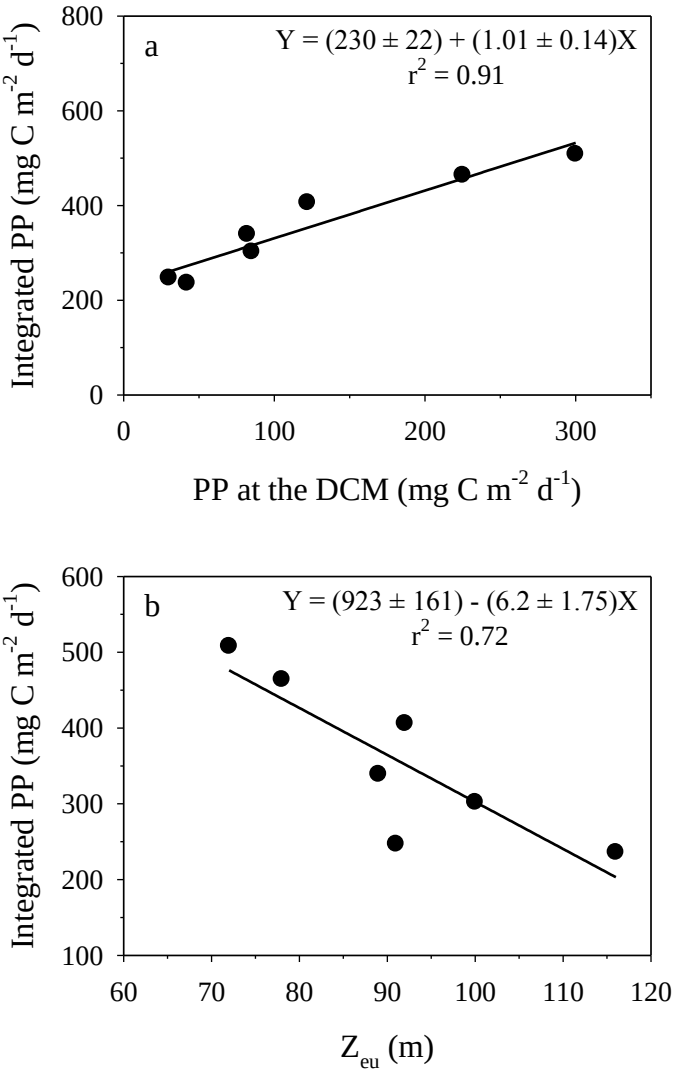

Fig. 8
Figueiras et al.

Figure(s)
Click here to download Figure(s): Fig 9.docx

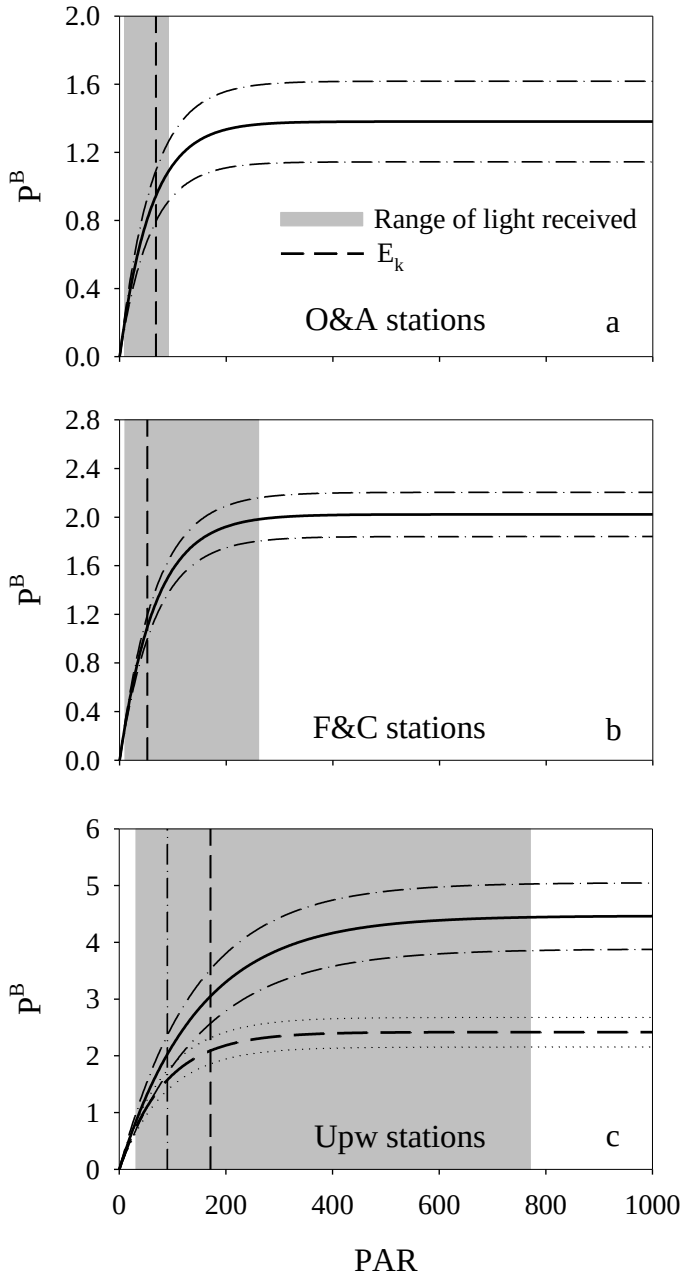

Fig. 9
Figueiras et al.